

Plasma Oxidation of Poly(cyclohexylmethylsilane) and Poly(phenylmethylsilane) Thin Films

J. L. C. Fonseca, C. P. Barker, and J. P. S. Badyal*

Department of Chemistry, Science Laboratories, Durham University, Durham DH1 3LE, England, U.K.

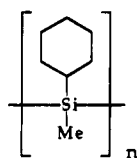
Received February 10, 1995; Revised Manuscript Received June 5, 1995[§]

ABSTRACT: Low-temperature glow discharge oxidation of poly(cyclohexylmethylsilane) and poly(phenylmethylsilane) thin films produces an SiO_xH_y -rich skin which blocks any further subsurface degradation. The rate and depth of oxygenation is found to be strongly influenced by the type of polysilane used.

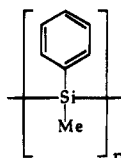
Introduction

Polysilane derivatives have interesting optical and semiconductive properties.¹⁻³ They are thermally and oxidatively stable, and yet are photochemically labile over a broad spectral range. The $-\text{Si}-\text{Si}-$ polymer backbone is σ -conjugated, and the $\sigma-\sigma^*$ electronic transition can be readily excited by UV laser irradiation, which in turn causes local cleavage of the polysilane polymer.⁴ This inherent characteristic of polysilanes makes them particularly suitable for multilayer resist schemes. These polymers are soluble in common organic casting solvents and can be coated as high-quality optical films. In the case of dry processing, UV laser ablation of the polysilane followed by exposure to a nonequilibrium oxygen glow discharge results in preferential stripping of any exposed underlying material, while remaining regions of polysilane polymer undergo oxidation to form an etch-resistant SiO_xH_y mask.^{5,6}

In this study, the susceptibilities of an aliphatic-substituted polysilane (poly(cyclohexylmethylsilane)) and an aromatic-substituted polysilane (poly(phenylmethylsilane)) toward oxygen glow discharge modification have been compared using X-ray photoelectron spectroscopy (XPS) and Fourier transform infrared spectroscopy (FTIR). Structurally, both polysilane polymers are identical apart from the former containing a saturated 6-membered ring, whereas the latter possesses a phenyl substituent instead.



Poly(cyclohexylmethylsilane) (PCHMS)



Poly(phenylmethylsilane) (PPMS)

Experimental Section

Poly(cyclohexylmethylsilane) ($T_g = 93^\circ\text{C}$) and poly(phenylmethylsilane) ($T_g = 112-122^\circ\text{C}$) (purchased from ABCR) were spin coated onto additive-free polyethylene film (Metal Box Co.) using 2% weight/volume toluene solution.⁷

Low-pressure oxygen plasma treatment was carried out in an electrodeless cylindrical reactor (4.5 cm diameter, 460 cm^3 volume, with a leak rate better than $4 \times 10^{-3} \text{ cm}^3 \text{ min}^{-1}$) enclosed in a Faraday cage.⁸ This was fitted with a gas inlet, a Pirani pressure gauge, and a 27 L min^{-1} two-stage rotary pump attached to a liquid nitrogen cold trap. A matching

network was used to inductively couple a copper coil (4 mm diameter, 9 turns, spanning 8–15 cm from the gas inlet) wound around the reactor to a 13.56 MHz radio frequency (rf) generator. All joints were grease-free. Gas and leak mass flow rates were measured by assuming ideal gas behavior.⁹ A typical experimental run comprised initially scrubbing the reactor with detergent, rinsing with isopropyl alcohol, and oven drying, followed by a 60 min high-power (50 W) air plasma cleaning treatment. At this stage, a piece of polysilane-coated polyethylene substrate was inserted into the center of the reactor (i.e., the glow region) and evacuated down to a base pressure of 1.5×10^{-3} Torr. Subsequently, oxygen was introduced into the reaction chamber at 1×10^{-1} Torr pressure and a flow rate (F_V) of $0.96 \text{ cm}^3 \text{ min}^{-1}$. After allowing 5 min for purging, the glow discharge was ignited at a predetermined power for 1 min. Upon termination of treatment, the rf generator was switched off, and the system was vented to the atmosphere.

X-ray photoelectron spectroscopy (XPS) characterization was carried out on a Kratos ES200 X-ray photoelectron spectrometer operating in the fixed retarding ratio (FRR, 22:1) mode. Ar^+ ion depth profiling studies were performed on a Vacuum Generators ESCALAB instrument, using constant analyzer energy mode photoelectron detection (CAE, 50 eV pass energy) and a cold cathode ion gun (VG AG21, 1–2% energy spread) for substrate etching. Magnesium $\text{K}\alpha$ X-rays (1253.6 eV) were used in both spectrometers, with an electron take-off angle of 30° to the substrate normal. A constant flux of 3 keV Ar^+ ions was maintained during depth profiling experiments by keeping the ion beam current fixed at 1.5 μA . An IBM PC was used for XPS data accumulation and component peak analysis (assuming linear background subtraction and Gaussian fits with fixed fwhm¹⁰). All binding energies are referenced to the hydrocarbon ($-\text{C}_2\text{H}_5-$) component at 285.0 eV.¹¹

Transmission infrared absorbance spectra were collected on a FTIR Mattson Polaris instrument.¹² Thin films of polysilane were spin coated onto pressed KBr disks. Typically, 100 scans were acquired at a resolution of 4 cm^{-1} .

Results

XPS. Polyethylene substrate was chosen since it has no oxygen content, thereby avoiding any possible confusion about the origins of any measured $\text{O}(1s)$ signal following oxygen plasma treatment. The main $\text{Mg K}\alpha_{1,2} \text{C}(1s)$ peak centered at a binding energy of 285.0 eV for both of the polysilanes (0 W) can be assigned to $\text{C}-\text{H}$, $\text{C}-\text{C}$ and $\text{C}-\text{Si}$ environments^{13,14} (Figures 1a and 2a). The $\text{C}(1s)$ feature shifted by approximately 9 eV toward lower binding energy can be attributed to the $\text{Mg K}\alpha_{3,4}$ satellite line. In the case of poly(phenylmethylsilane), there was an additional weak $\text{C}(1s)$ component around 291.6 eV having an area of 3% of the main $\text{C}(1s)$ peak; this exhibited a Gaussian profile of different fwhm

* To whom correspondence should be addressed.

[§] Abstract published in *Advance ACS Abstracts*, August 1, 1995.

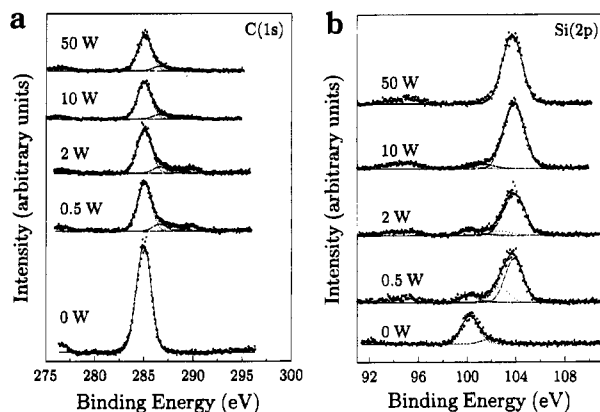


Figure 1. XPS spectra of oxidized poly(cyclohexylmethylsilane) polymer as a function of oxygen glow discharge power: (a) C(1s); (b) Si(2p).

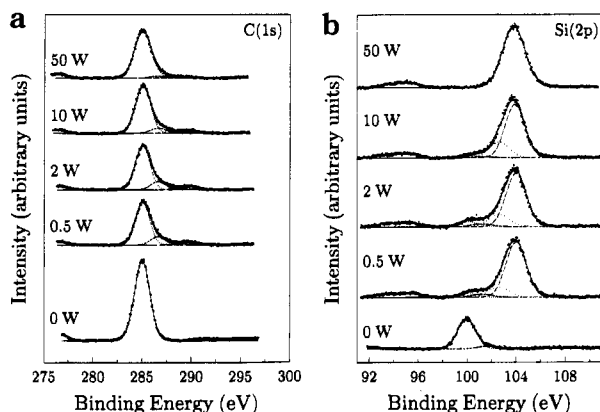


Figure 2. XPS spectra of oxidized poly(phenylmethylsilane) polymer as a function of oxygen glow discharge power: (a) C(1s); (b) Si(2p).

relative to the main peak and can be attributed to $\pi-\pi^*$ shake-up transitions accompanying core level ionization of the aromatic rings.¹⁵ For both polysilanes only one major type of Si(2p) core level environment at 100.0 eV was detected; this is characteristic of the $-(R_1)Si(R_2)_n-$ structure² (Figures 1b and 2b). A weak shoulder at 101.8 eV was discernible (less than 1%) and could be attributed to either the occurrence of silicon atoms adjacent to a carbon atom rather than a silicon center along the polymeric backbone or slight oxidation at the polymer surface. For both polysilane polymers, the O(1s) intensity was less than 1%.

Plasma oxidation of each type of polysilane spin coated onto polyethylene substrate was studied as a function of glow discharge power (Figures 1 and 2). This treatment was found to be very effective down to the depths accessible by XPS (5–20 Å). Using instrumentally determined sensitivity factors for C(1s):O(1s):Si(2p) equal to 1.00:0.55:1.05, a plateau in the elemental concentrations is reached well below 5 W corresponding to 30% carbon, 35% silicon, and 35% oxygen for the poly(cyclohexylmethylsilane) polymer and 41% carbon, 31% silicon, and 28% oxygen for the corresponding poly(phenylmethylsilane) material (Figures 3 and 4). The aliphatic polysilane yields a higher level of oxidation at the surface compared to its aromatic counterpart, while the latter reaches its limiting elemental percentages at lower glow discharge powers. Clearly, this analysis excludes any hydrogen content, since it cannot be detected by XPS.¹⁶ During plasma oxidation, the Si(2p) peak gains intensity and shifts by approximately 3.7 eV toward higher binding energy. The Si(2p)

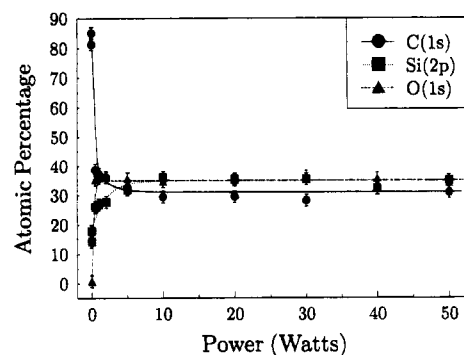


Figure 3. Compositional variation of poly(cyclohexylmethylsilane) polymer as a function of oxygen glow discharge treatment (neglecting hydrogen content).

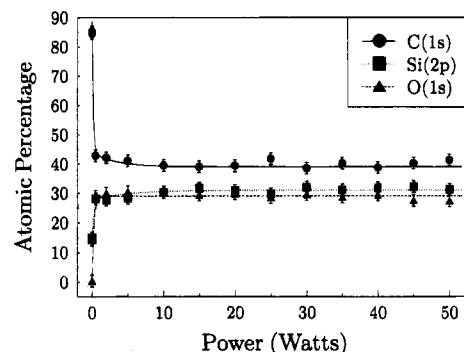


Figure 4. Compositional variation of poly(phenylmethylsilane) polymer as a function of oxygen glow discharge treatment (neglecting hydrogen content).

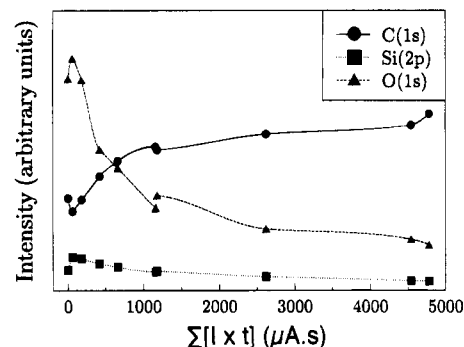


Figure 5. Ar⁺ ion depth profile study of oxygen glow discharge treated (50 W) poly(cyclohexylmethylsilane) polymer.

envelope could be fitted to Si–Si (100.1 eV), Si–H/Si–C (101.2 eV), Si–[OC_xH_y]_n (102.6 eV), and O–Si–O (104.0 eV) silicon centers.¹⁷ In addition, the main C(1s) peak becomes attenuated together with the emergence of a weak oxidized shoulder at high binding energy, which can be taken as a convolution of $\geq C-CO_2-$ (285.7 eV), $\geq C-O-$ (286.6 eV), $\geq C=O/-O-C-O-$ (287.9 eV), $-O-C=O$ (289.0 eV), and $-O-CO-O-$ (290.4 eV) functionalities.¹⁸ In both cases no shrinkage in polymer was observed.

Passage of oxygen over each polysilane polymer in the absence of a glow discharge resulted in negligible surface oxidation.

XPS in conjunction with Ar⁺ ion depth profiling of the oxidized polysilane layers confirmed the buildup of oxygenated silicon species in the near-surface region (Figures 5 and 6). The O(1s) profiles show that the level of oxidation decays in both gradually with depth. This is most likely due to permeation of glow discharge generated oxygen species into the subsurface region

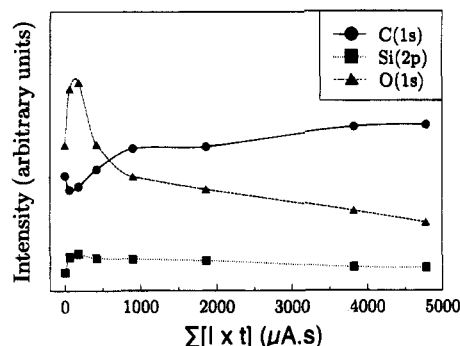


Figure 6. Ar^+ ion depth profile study of oxygen glow discharge treated (50 W) poly(phenylmethylsilane) polymer.

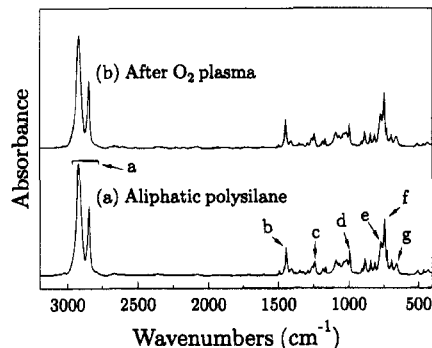


Figure 7. Transmission FTIR spectra of poly(cyclohexylmethylsilane): (a) clean; (b) oxygen glow discharge treated (50 W).

during the early stages of plasma treatment, when reactive ion etch barrier will be poor. Although the aromatic polysilane is less oxygen-rich at the surface, it has in fact oxidized down to a deeper level.

FTIR. Clean poly(cyclohexylmethylsilane) exhibits strong infrared absorbances related to $^{19}\text{C-H}$ stretching in CH_3 and CH_2 (a: 2920 and 2847 cm^{-1}), $-\text{CH}_2-$ bending (b: 1447 cm^{-1}), CH_3 bending in SiCH_3 (c: 1244 cm^{-1}), C-C stretching (d: 995 cm^{-1}), CH_3 rocking in SiCH_3 (e: 774 cm^{-1}), $-\text{CH}_2-$ rocking (f: 745 cm^{-1}), and Si-C stretching (g: 661 cm^{-1}) (Figure 7). The phenyl-substituted polysilane polymer displayed the following absorbances:¹⁹ aromatic C-H stretching (h: 3067 , 3050 , and 2993 cm^{-1}), methyl C-H stretching (i: 2957 and 2895 cm^{-1}), C-C ring stretching (j: 1483 cm^{-1}), C-H bending (k: 1427 cm^{-1}), CH_3 bending in SiCH_3 (l: 1247 cm^{-1}), monosubstituted benzene (m: 1099 cm^{-1}), CH_3 rocking in SiCH_3 (n: 781 cm^{-1}), out-of-plane C-H bending (o: 754 and 729 cm^{-1}), ring C-C bending (p: 696 cm^{-1}), Si-C stretching (q: 667 cm^{-1}), out-of-plane C-C ring bending (r: 463 cm^{-1}) (Figure 8).

Glow discharge oxidation of poly(phenylmethylsilane) resulted in the appearance of absorbances related to Si-O-Si and/or Si-O-C stretches²⁰ (s: 1130 – 990 cm^{-1}). However, such Si-O-Si and/or Si-O-C stretches (s: 1130 – 990 cm^{-1}) were absent for the treated poly(cyclohexylmethylsilane) polymer; this is consistent with the deeper level of oxidation measured by XPS for the former during Ar^+ ion depth studies.

Discussion

A pure oxygen plasma contains ions, atoms, ozone, and metastables of atomic and molecular oxygen as well as electrons and a broad electromagnetic spectrum.²¹ This highly reactive medium readily leads to oxidation at a polysilane surface. In the case of conventional hydrocarbon polymers, phenyl-containing chains are

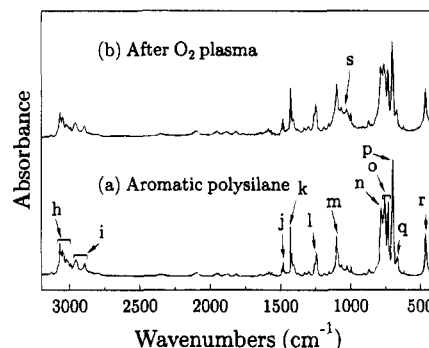


Figure 8. Transmission FTIR spectra of poly(phenylmethylsilane): (a) clean; (b) oxygen glow discharge treated (50 W).

Table 1. Quantum Yield Data for Poly(cyclohexylmethylsilane) (PCHMS) and Poly(phenylmethylsilane) (PPMS)^{25,26}

polysilane	solvent	λ (nm)	solution		solid film	
			$\Phi(s)^a$	$\Phi(x)^a$	$\Phi(s)$	$\Phi(x)$
PCHMS	toluene	355	1.2	0.06	0.022	0.000
PPMS	THF	313	0.97	0.12	0.015	0.002

^a $\Phi(s)$ is the quantum yield for scission and $\Phi(x)$ is the quantum yield for cross-linking.

more resistant to plasma etching than their aliphatic analogues²² due to the stabilization of oxygenated aromatic intermediates for the former, while chain scission reactions forming volatile species are predominant for the latter.^{23,24} Poly(cyclohexylmethylsilane) ($\lambda_{\text{max}} = 320\text{ nm}$) and poly(phenylmethylsilane) ($\lambda_{\text{max}} = 337\text{ nm}$) both absorb the ultraviolet radiation generated by the oxygen plasma and thereby undergo scission and cross-linking, which is accompanied by surface oxidation. Table 1 summarizes some reported quantum yield data for the two polysilane polymers used in this investigation. It can be seen that the aliphatic polysilane has a greater tendency to undergo scission than the aromatic one, while the latter polymer cross-links more easily. From this data, one would expect a greater buildup of SiO_xH_y species in the case of the poly(cyclohexylmethylsilane) polymer, since its aliphatic hydrocarbon side groups can only undergo rupture or oxidation, whereas in the case of poly(phenylmethylsilane), the phenyl rings in the parent polymer will participate in cross-linking as well as rupture and oxidation, resulting in a slower loss of carbon and therefore a poorer resistance toward the penetration of reactive oxygen species into the subsurface during plasma oxidation. The aforementioned description is consistent with the XPS, Ar^+ ion depth profiling, and FTIR results, where the concentration of SiO_xH_y moieties at the surface is found to be greatest for poly(cyclohexylmethylsilane), while poly(phenylmethylsilane) is oxidized to a greater depth.

Conclusions

A thin SiO_xH_y -rich skin is formed during low-pressure oxygen glow discharge treatment of poly(cyclohexylmethylsilane) and poly(phenylmethylsilane) thin films. The type of substituents along the polysilane backbone can strongly influence the plasma oxidation chemistry. Aliphatic side groups are more readily lost than aromatic substituents and therefore yield a thinner, but more SiO_xH_y -rich layer.

Acknowledgment. J.L.C.F. thanks Brazil's Conselho Nacional de Desenvolvimento Científico e Tecnológico for financial support.

lógico for financial support and SERC for provision of equipment during the course of this work.

References and Notes

- (1) Miller, R. D.; MacDonald, S. A. *J. Imaging Sci.* **1987**, *31*, 43.
- (2) Miller, R. D. *Chem. Rev.* **1989**, *89*, 1359.
- (3) Miller, R. D. *Angew. Chem., Int. Ed. Engl. Adv. Mater.* **1989**, *28*, 1733.
- (4) Kunz, R. R.; Horn, M. W.; Wallraff, G. M.; Bianconi, P. A.; Miller, R. D.; Goodman, R. W.; Smith, D. A.; Eshelman, J. R.; Ginsberg, E. J. *Jpn. J. Appl. Phys.* **1992**, *31*, 4327.
- (5) Miller, R. D.; Hofer, D.; Fickes, G. N.; Willson, C. G.; Marinero, E. E.; Trefonas, P.; West, R. *Polym. Eng. Sci.* **1986**, *26*, 1129.
- (6) Reichmanis, E.; Smolinsky, G.; Wilkins, C. W., Jr. *Solid State Technol.* **1985**, *28*, 130.
- (7) Bunshah, R. F.; Blocker, J. M.; Bonifield, T. D.; Fish, J. G.; Ghate, P. B.; Jacobson, B. E.; Mattox, D. M.; McGuire, G. E.; Schwartz, M.; Thornton, J. A.; Tucker, R. C. In *Deposition Technologies for Films and Coatings*; Noyes Publications: New Jersey, 1982; p 511.
- (8) Shard, A. G.; Badyal, J. P. S.; *Macromolecules* **1992**, *25*, 2053.
- (9) Johansson, G.; Hedman, J.; Berndtsson, A.; Klasson, M.; Nilsson, R. *J. Electron Spectrosc.* **1973**, *2*, 295.
- (10) Evans, J. F.; Gibson, J. H.; Moulder, J. F.; Hammond, J. S.; Goretzki, H. *Fresenius Z. Anal. Chem.* **1984**, *319*, 841.
- (11) Johansson, G.; Hedman, J.; Berndtsson, A.; Klasson, M.; Nilsson, R. *J. Electron Spectrosc.* **1973**, *2*, 295.
- (12) Fonseca, J. L. C.; Apperley, D. C.; Badyal, J. P. S. *Chem. Mater.* **1993**, *5*, 1676.
- (13) Inagaki, N.; Katsuoka, D. *J. Membr. Sci.* **1987**, *34*, 297.
- (14) Gray, R. C.; Carver, J. C.; Hercules, D. M. *J. Electron Spectrosc.* **1976**, *8*, 343.
- (15) Clark, D. T.; Dilks, A. *J. Polym. Sci., Polym. Chem. Ed.* **1977**, *15*, 15.
- (16) Beamson, G.; Briggs, D. *High Resolution XPS of Organic Polymers: The Scienta ESCA300 Database*; J. Wiley & Sons: Chichester, 1992.
- (17) Laoharojanaphand, P.; Lin, T. J.; Stoffer, J. O. *J. Appl. Polym. Sci.* **1990**, *40*, 369.
- (18) Clark, D. T.; Dilks, A. *J. Polym. Sci., Polym. Chem. Ed.* **1978**, *16*, 991.
- (19) Graf, R. T.; Koenig, J. L.; Ishida, H. Introduction to Optics and Infrared Spectroscopic Techniques. In *Fourier Transform Infrared Characterization of Polymers*; Ishida, H., Ed.; Plenum Press: New York, 1987.
- (20) Fonseca, J. L. C.; Badyal, J. P. S. *Macromolecules* **1992**, *25*, 4730.
- (21) Hollahan, J. R.; Bell, A. T., Eds. *Techniques and Applications of Plasma Chemistry*; Wiley: New York, 1974.
- (22) *Plasma Deposition, Treatment, and Etching of Polymers*; d'Agostino, R., Ed.; Academic Press, Inc.: San Diego, 1990; p 367.
- (23) Taylor, C. S.; Wolf, T. M. *Polym. Eng. Sci.* **1980**, *20*, 1087.
- (24) Cain, S. R.; Egitto, F. D.; Emmi, F. *J. Vac. Sci. Technol.* **1987**, *A5*, 1578.
- (25) Miller, R. D.; Guillet, J. E.; Moore, J. *Polym. Prepr. (Am. Chem. Soc., Div. Polym. Chem.)* **1988**, *29*, 552.
- (26) Hofer, D. C.; Miller, R. D.; Willson, C. G. *Adv. Resist. Technol.* **1984**, *469*, 16.

MA9501656